Attenuation lengths of low-energy electrons in solids derived from the yield of proton-excited Auger electrons: beryllium and aluminum

C. J. Powell and R. J. Stein*

National Bureau of Standards, Washington, D. C. 20234

P. B. Needham, Jr. and T. J. Driscoll

College Park Metallurgy Research Center, Bureau of Mines, U. S. Department of the Interior, College Park, Maryland 20740
(Received 9 August 1976)

Values are reported for the absolute yields of KVV Auger electrons from beryllium and $L_{23}VV$ Auger electrons from aluminum excited by 60- to 220-keV proton bombardment. The measurements were made using semi-infinite evaporated samples, and the results were used to derive effective values of the inelastic attenuation lengths for low-energy Auger electrons in the surface regions of the samples. The attenuation lengths determined using this technique were 6.1 Å for 100-eV electrons in Be and 1.9 Å for 67-eV electrons in Al. These effective attenuation lengths are appropriate for use in Auger-electron spectroscopy and x-ray photoelectron spectroscopy.

I. INTRODUCTION

The attenuation length, or total inelastic mean free path, of low-energy electrons in solids is an important parameter required for the quantitative analysis of surfaces by Auger-electron spectroscopy (AES) and x-ray photoelectron spectroscopy (XPS).[1] The electron energies of practical interest for AES and XPS are usually between 50 and 2000 eV, and the attenuation lengths can range from 3 to 100 Å, depending on the material and the electron energy. Techniques for measuring attenuation lengths have been discussed in a recent review[1] where it was pointed out that each method contains one or more sources of systematic error that are particularly troublesome when the shorter attenuation lengths (<20 Å) are to be determined. Further, it is usually difficult to estimate the magnitude of the various systematic errors and to make appropriate corrections.

In this paper we report the results of experiments to measure electron attenuation lengths in solids by a method suggested by Musket and Bauer.[2] The basis of the method is the generation of a calculable source of electrons, in this case Auger electrons, in a semi-infinite sample by proton bombardment. The Auger-electron yield is measured and the electron attenuation length in the sample (at the Auger-electron energy) is determined with the use of a simple model to describe Auger-electron transport from the solid to an external detector. We present here attenuation-length determinations for evaporated semi-infinite samples of beryllium and aluminum; a preliminary report of this work was presented earlier.[3]

Electron attenuation lengths in Be and Al were determined using 160-keV protons to remove electrons from the K shell in Be and from the L shell in Al. The yields of the Auger electrons associated with the KVV (V = valence) and $L_{23}VV$ transitions that occur at about 100 eV in Be and 67 eV in Al, respectively, were measured. Proton bombardment of Al causes additional (albeit fewer) ionizations from the L_1 subshell, but L_1 vacancies predominantly decay by Coster-Kronig transitions thereby transferring the L_1-subshell vacancies to the L_{23} subshells.[4]

Electron attenuation-length determinations can also be made in a similar manner with other forms of excitation if the appropriate cross sections for electron generation are known. Results of similar experiments in which the Auger electrons were produced by electron bombardment are to be reported later.[5] X rays could be used to produce electrons by photoionization, but the greater difficulty in measuring the incident x-ray flux (compared with the simple measurement of proton or electron currents) makes this variation of the experiment less attractive. Relative values of attenuation lengths can, however, be obtained from a comparison of photoelectron and Auger-electron currents (associated with the same core excitation) in an XPS experiment.[6]

The determination of electron attenuation lengths from the yield of either proton- or electron-excited Auger electrons also suffers from several sources of systematic error (to be described below) that are difficult to estimate. The present experiment was undertaken, nevertheless, for several reasons:

(i) The method described here is well suited for the measurement of short attenuation lengths ($\lesssim 10$Å). Most previous measurements of attenuation lengths have been made by the so-called

"overlayer" method[1] for which the morphological characterization of thin layers (of thickness comparable to the attenuation length) is necessary but very difficult.

(ii) Present methods for quantitative surface analysis by AES and XPS make use of the same simple transport model that is used here.[7] Although this model is not expected to be valid in detail because of the neglect of diffraction effects, the results of the present experiment can at least be used as empirical parameters in AES and XPS experiments. Also, the use of semi-infinite samples simulates the practical situation encountered in AES and XPS.

(iii) Comparison of attenuation-length data obtained by different techniques can be used to set reasonable bounds on the magnitude of the relevant systematic errors in any particular experiment. Also, experimental data of known reliability are required in order to check the validity of recent theoretical calculations of electron attenuation lengths.[4,8]

The experimental method used here is described in Sec. II. Details of the apparatus and experimental procedure are reported in Sec. III. The measured yields of Auger electrons from Be and Al, as well as the derived attenuation lengths, are presented and discussed in Sec. IV.

II. ANALYSIS OF EXPERIMENTAL METHOD

We consider the geometry shown in Fig. 1 where a current I_p of protons with energy E_p is incident on a semi-infinite elemental sample at an angle β with respect to the surface normal. In this experiment, the Auger electrons that are detected externally originate predominantly (at least 99% of the signal) from a depth less than 100 Å (if the electron attenuation length is less than about 20 Å). To reach this depth, the incident protons have traversed approximately 300 Å when $\beta = 70°$, the value for our experiment. For protons with en-
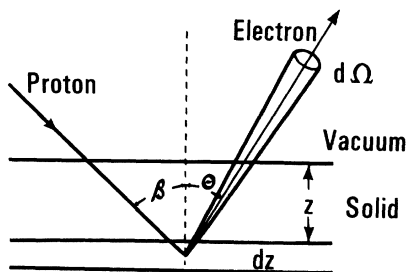

FIG. 1. Schematic outline of the model geometry for the present experiment (with protons incident on, and Auger electrons exiting from the sample).

ergies between 60 and 220 keV, the average energy loss in Be and Al would be between 3.1 and 3.8 keV over a path of 300 Å.[9] It is, therefore, reasonable to neglect the variation of the inner-shell ionization cross section with proton energy, particularly since the ionization cross section does not vary rapidly with energy in the proton energy region of interest here and since the attenuation lengths for Be and Al are expected to be less than 20 Å.[1]

The rate of ionization R_0 of a particular inner shell in an incremental thickness dz at depth z into the solid is

$$R_0 = N\sigma_i I_p dz/\cos\beta, \tag{1}$$

where σ_i is the cross section for ionization at the proton energy E_p and N is the number density of atoms in the solid. If there is no significant vacancy redistribution in the ionized atom caused by Coster-Kronig processes, the number of Auger electrons per second produced by the decay of the initial inner-shell vacancies R_A is

$$R_A = (1 - \omega)R_0, \tag{2}$$

where ω is the fluorescence yield for the shell or subshell of interest. Equations (1) and (2) can be readily generalized to the case where the incident protons cause vacancies in two or more subshells that directly or indirectly produce (by Auger or Coster-Kronig processes) the Auger electrons of interest. Also, a distinction may have to be made experimentally between Auger electrons at the "normal" energy and the "satellite" Auger electrons originating from atoms with multiple initial vacancies or from atoms with particular additional excitations.[10]

The probability P of an Auger electron emerging from the solid without inelastic scattering in a solid angle $d\Omega$ at an angle θ with respect to the surface normal is

$$P = [\exp(-z/\lambda \cos\theta)] d\Omega/4\pi, \tag{3}$$

where λ is the total inelastic mean free path or attenuation length in the sample for electrons at the particular Auger-electron energy. Equation (3) is based on the implicit assumption that the effects of elastic scattering in the sample are negligible, an assumption believed to be valid to first order for an amorphous or polycrystalline sample.[1] It has also been assumed that the probability of inelastic scattering per unit path length in the sample is a constant (characterized by λ) throughout the sample up to the surface; this assumption will be discussed in Sec. IV.

The total Auger-electron current $I_A(\theta)$ in the direction θ is obtained by combining Eqs. (1)–(3) and performing the integration over z from zero

to an effective upper limit of infinity.

$$I_A(\theta) = \int R_A P = \frac{N\sigma_i I_p \lambda(1-\omega)\cos\theta\, d\Omega}{4\pi\cos\beta} \quad (4)$$

The total Auger-electron current collected by the external electron-energy analyzer is obtained by an integration over the appropriate solid angle. With our experimental arrangement, shown in Fig. 2, electrons are detected with a four-grid retarding-field analyzer (RFA) oriented with its axis at an angle of 20° with respect to the sample normal. This analyzer can detect electrons emitted at angles between 4.2° (due to an internal gun in the analyzer) and 48° with respect to the analyzer axis. The overall collection efficiency T of the RFA is determined by the transmission through the grids and the collector efficiency. The measured Auger-electron current I_m can then be written

$$I_m = GTN\sigma_i I_p \lambda(1-\omega), \quad (5)$$

where the factor $G = 0.376$ is determined from the angular integration for our geometry. Therefore, the attenuation length

$$\lambda = \frac{I_m}{GTN\sigma_i I_p(1-\omega)} \quad (6)$$

can now be determined from the measured yield Y of Auger electrons $(Y = I_m/I_p)$, the instrumental constants T and G, and the sample parameters N, σ_i, and ω.

III. APPARATUS

A schematic of the present experimental arrangement is shown in Fig. 2. Protons were produced in an rf ion source, accelerated to energies between 60 and 220 keV, and directed to the experimental chamber as described previously.[11] The beam diameter at the sample was about 1.7 mm while the divergence was about 1.7×10^{-3} rad. The
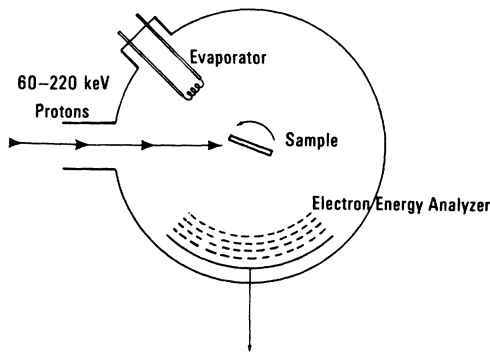

FIG. 2. Schematic outline of experimental arrangement.

proton current to the target was determined with a bias of +300 V applied to the target; previous experiments[11] have indicated that this method of current measurement yields a value of the proton current that is about 6% too high.

The sample substrate could be rotated to face a tungsten-filament evaporator. During evaporation, a shield was used to protect the analyzer, and during each evaporation cycle at least several hundred angstroms of sample were deposited on the substrate.

The retarding-field analyzer was part of a commercial four-grid low-energy electron diffraction and Auger-electron system operated for the most part in the conventional manner. A 5-kHz sinusoidal voltage was superimposed on the dc retarding voltage to obtain both the energy distribution of electrons entering the analyzer as well as the derivative of the energy distribution. The screen (collector) of the analyzer was operated at a potential of +300 V with respect to ground and was coupled through a high-transimpedance preamplifier[12] to a lock-in amplifier.

If we assume, for the moment, that the measured electron energy distribution consists of a single Auger-electron peak with Gaussian shape superimposed on a constant background, the current within the peak I_m can be obtained from Taylor's formula[13]

$$I_m = 2.5\sqrt{2}\ V_1\sigma/kZ, \quad (7)$$

where σ is the standard deviation of the Gaussian-shaped peak (full width at half maximum is 2.36σ), V_1 is the rms output voltage (above the background) of the preamplifier at the modulation frequency when the analyzer retarding voltage is adjusted to detect the maximum of the Gaussian peak, k is the amplitude of the modulation voltage applied to the analyzer, and Z is the transimpedance of the preamplifier. Equation (7) has been shown[13] to have an error of about 1% if $k/\sigma = 0.3$, the ratio generally applicable to data acquired here. The practical problem of determining I_m when the Auger peak in the measured electron energy distribution is not Gaussian will be discussed in Sec. IV.

The Auger current can also be obtained from the derivative of the energy distribution from[13]

$$I_m = 8.33\sqrt{2}\ V_2\sigma^2/k^2 Z, \quad (8)$$

where V_2 is the difference between the maximum and minimum in the rms output voltage of the preamplifier at the second harmonic of the modulation frequency when the analyzer retarding voltage is scanned through the voltage region of the peak. In the work reported here, this form of Taylor's equation was used only for obtaining the variation of the Auger-electron yields as a function of pro-

ton energy and for determining the effect of
elapsed time between evaporation of a fresh
sample and making the Auger measurement.
Equation (8) is convenient for the determination of
relative values of I_m but absolute values of I_m can
be obtained with greater accuracy from Eq. (7).

The principal sources of error in this experi-
ment are associated with the value of σ_i in Eq. (6)
and the determination of I_m. Since several sources
of error were large ($\approx 20\%$) and could not be
easily eliminated or minimized, values of several
percent for the accuracy and precision in other
quantities were considered adequate.

The current-measuring system was calibrated
with an accuracy of about 2%. The transmission
of the analyzer grids and the screen collection
efficiency, represented together by the parameter
T in Eqs. (5) and (6), were determined by mounting
an electron gun opposite the analyzer. The beam
could be deflected to enter a Faraday cup or it
could be deflected to different regions of the an-
alyzer screen. The average value of T was found
to be 0.47 with an uncertainty (probable error) of
2%.

IV. RESULTS AND DISCUSSION

A. Absolute Auger-electron yield for $E_p = 160$ keV

Figure 3 shows typical Auger spectra obtained
for Be and Al with a proton beam energy E_p of
160 keV. These spectra do not differ significantly
from those obtained with electron excitation.[5,14,15]
During the course of any given series of measure-
ments (for example, recording the Auger spectra
as a function of the proton energy), fresh evapora-
tions were made at suitable intervals to minimize
the effects of adsorbed contaminants on the Auger
spectra. Even though the total pressure in the
specimen region was typically 10^{-7} Pa (about 10^{-9}
Torr), except during evaporations when the pres-
sure sometimes rose to 10^{-6} Pa (about 10^{-8} Torr),
the Auger spectra did not change significantly over
10- to 30-min intervals (which were large compar-
ed with the measurement time of 1–2 min for an
individual Auger spectrum).

In Fig. 3 the Auger-electron feature of interest
is superimposed on a background of low-energy
secondary electrons and also overlaps with struc-
ture that is predominantly associated with inelas-
tic scattering of the Auger electrons. Sickafus[16]
and Houston[17] have developed analog and digital
procedures, respectively, for isolating Auger-
electron features (characterized by relatively
small radii of curvature in the secondary-electron
energy distribution) from the secondary electron
background (characterized by relatively large radii
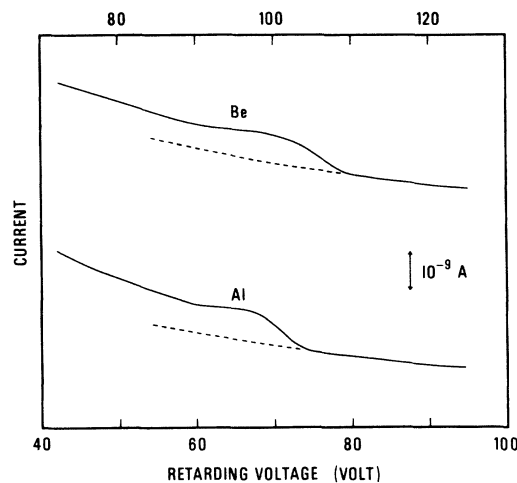of curvature). Mularie and Peria[18] and Houston

FIG. 3. Typical Auger-electron spectra measured
from Be (top) and Al (bottom) when the samples were
bombarded by 160-keV protons. These spectra are the
measured first derivative of the current collected by
the retarding-field analyzer. The ordinate is V/Z in
Eq. (7), the proton current was 1.2 μA for both spectra,
and k was equal to 2 V for Be and 1.5 V for Al. The
dashed line shows the extrapolated background used to
determine the Auger-electron peak amplitude.

and Madden[19] have shown that the net Auger-elec-
tron signal can be deconvoluted with an appropriate
electron energy-loss spectrum to yield a line
shape characteristic of the noninelastically
scattered Auger electrons. For the case of the
$L_{23}VV$ Auger-electron transition in Al, of interest
here, Houston[19] has shown that the characteristic
line shape is a single peak with some asymmetry.

In light of this information and because of the
other sources of error in determining λ, we have
used the following approximation as a procedure
to determine I_m. The secondary-electron back-
ground at energies higher than the Auger-electron
feature was extrapolated to lower energies in the
manner indicated by dashed lines in Fig. 3; in
essence, it has been assumed that the background
under the peak of interest can be determined with
sufficient accuracy by a smooth extrapolated curve
over an energy range of about 15 eV. Then, at
about 100 eV for Be and at about 67 eV for Al, we
measured the maximum amplitude [V_1 in Eq. (7)]
from the background to the peak. The limit of
error in the determination of this amplitude (ow-
ing to the uncertainty in background location) is
believed to be ±5%. We determined peak ampli-
tudes from spectra obtained with a proton energy
of 160 keV and a proton beam current of about
1 μA. A value of σ was found from the high-energy
(essentially undistorted) half of the measured line
shape and Eq. (7) was then used to obtain prelimi-

TABLE I. Summary of parameters used in Eqs. (6) and (7) to determine the attenuation length in Be and Al. Estimated probable errors are shown in parentheses (Sec. IV C). The values for Y and for the inner-shell ionization cross sections are for a proton energy of 160 keV, and the values of attenuation lengths λ refer to electrons of the characteristic Auger-electron energy E_A for each metal.

Parameter	Be	Al
$Y=I_m/I_p$	8.0×10^{-3} ($\pm10\%$)	8.7×10^{-3} ($\pm10\%$)
Z (Ω)	10^7 ($\pm 5\%$)	10^7 ($\pm 5\%$)
σ (V)	5.9 ($\pm 2\%$)	4.0 ($\pm 2\%$)
k (V)	2 ($\pm 2\%$)	1 to 2 ($\pm 2\%$)
T	0.47 ($\pm 2\%$)	0.47 ($\pm 2\%$)
σ_i (cm^2)	6×10^{-18}	4.2×10^{-17}
N (cm^{-3})	1.24×10^{23}	6.0×10^{23}
G	0.376	0.376
E_A (eV)	100	67
λ (Å)	6.1	1.9

nary values of I_m and of the yield $Y=I_m/I_p$.

We have assumed in the use of Eq. (7) that the Auger-electron feature of interest was a symmetrical, Gaussian peak. Although the line shape of the high-energy side of the observed peak was not exactly Gaussian, we estimate that the limit of error in I_m on this account to be less than $\pm5\%$. We now proceed to estimate corrections to the preliminary values of I_m and Y to take account of inelastic scattering and of asymmetry of the Auger-electron peaks.

The shape of the measured Auger-electron energy distribution both at the peak and at higher energies can be shown by convolution calculations not to be distorted by more than about 5% by inelastic scattering (from considerations of the energies, line shapes, and expected relative intensities of volume and surface plasmons in Be and Al).[19-21] We have, therefore, reduced the preliminary yields by 5% (with an uncertainty of $\pm2\%$) to obtain new yields corresponding to noninelastically scattered Auger electrons.

Houston[19] has corrected a measured $L_{23}VV$ Al Auger-electron spectrum for inelastic electron scattering and has found that the "true" line shape is asymmetrical. The intensity on the low-energy side of the peak was found to be 50% greater than that of the high-energy side. We have therefore increased the yield determined for Al by 25% to account for this asymmetry. The true Auger-electron line shape for Be is not known but, since Be is a free-electron metal like Al, we believe that a comparable degree of asymmetry may exist for Be. However, the Be Auger-electron transition originates with a K-shell vacancy (in contrast to an L_{23}-shell vacancy for Al), and this difference

could lead to a different degree of asymmetry. The convolution calculations described above and comparisons of the spectra for Be and Al in Fig. 3 indicate that the peak asymmetry for Be is not likely to be greater than that for Al. We have, therefore, chosen to increase the yield for Be by only $12\frac{1}{2}\%$ to account for an expected asymmetry and assigned this value an additional error of $\pm12\frac{1}{2}\%$. The final corrected yields for Al and Be at the proton energy of 160 keV are given in Table I.

Finally, we note that I_m can also be determined from the derivative of the Auger-electron energy distribution, the form in which AES data is often acquired. Here, the distoring effects of inelastic scattering on the observed spectra can be minimized by measuring the negative-peak to background difference (corresponding to the undistorted high-energy side of the Auger-electron feature previously discussed) rather than the more commonly used negative-peak to positive-peak difference. Values of I_m obtained this way [with Eq. (8)] were consistent with those obtained from the energy distribution [with Eq. (7)], but had larger uncertainties than the latter due to the quadratic dependence of I_m on σ.

B. Auger-electron yield vs proton energy and proton-impact ionization cross sections

In this subsection we present measurements of the relative Auger-electron yield as a function of the incident proton energy and compare these measurements with ionization cross-section data. We then describe our selection of preferred values of σ_i to determine attenuation lengths with the use of Eq. (6).

We measured the relative Auger yields as a function of proton energy to ensure that the variation of yield followed the variation of ionization cross section (as would be expected from the analysis of Sec. II). The relative Auger-electron yields were determined with the use of Eq. (8) and were subsequently normalized to an absolute scale using the absolute yields obtained for $E_p = 160$ keV. It was experimentally convenient to measure absolute yields at $E_p = 160$ keV since at this energy the yields were close to their maximum values.

The variation of the yield Y as a function of proton energy between 60 and 220 keV is shown in Figs. 4(a) and 5(a) for Be and Al, respectively. These yield measurements are compared with corresponding measurements and calculations of proton-induced ionization cross sections σ_i as a function of E_p in Figs. 4(b) and 5(b).

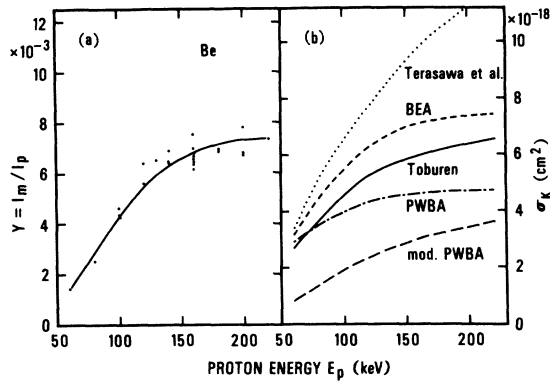We are aware of only one experiment in which K-shell ionization cross sections σ_K for Be by

FIG. 4. (a) Variation of the Auger-electron yield Y $=I_m/I_p$ for Be as a function of proton energy E_p. The solid line is a smooth curve through the experimental points. (b) Variation of σ_K for Be as a function of E_p. The short-dashed curve denoted BEA is calculated from the binary-encounter approximation (Ref. 25), the dot-dashed curve denoted PWBA from the plane-wave Born approximation (Refs. 27 and 28), and the long-dashed curve denoted mod. PWBA from the modified plane-wave Born approximation (Ref. 28). The dotted curve represents measurements of Terasawa et al. (Ref. 22) and the solid curve represents values of σ_K for Be derived from the experiment of Toburen (Ref. 24) as described in the text.

proton bombardment have been reported, that of Terasawa et al.[22] These values were obtained from measurements of proton-excited x-ray yields to give the x-ray production cross sections σ_x and a previous experimental determination[23] of the fluorescence yield, ω_K, that had an estimated uncertainty of about ±20%. For 160-keV protons, a value of $\sigma_K = 9.8 \times 10^{-18}$ cm^2 is obtained. Toburen[24] has measured the Auger-electron yield due to proton bombardment of gases containing low-Z elements (B,C,N,O,F,Ne), and his derived cross sections appear to lie on a common curve (with an imprecision of about 10%) when scaled as suggested by results from the binary-encounter approximation (BEA).[25] We have used the BEA to derive effective values of σ_K for Be from Toburen's data, and these are shown as a solid line in Fig. 4(b). Similar measurements for C and N have been made by Stolterfoht et al.[26] that agree with Toburen's data. A value of $\sigma_K = 6 \times 10^{-18}$ cm^2 for 160-keV protons can be derived from the curve for Be based on Toburen's data.

We also show in Fig. 4(b) the results of three theoretical calculations of σ_K for Be. The short-dashed line is calculated from the BEA of Garcia et al.[25] and yields a value for 160-keV protons of $\sigma_K = 7.1 \times 10^{-18}$ cm^2. The dot-dashed line in Fig. 4(b) is from the plane-wave Born approximation (PWBA) by Khandelwal et al.[27,28] and yields a

value for 160-keV protons of $\sigma_K = 4.6 \times 10^{-18}$ cm^2. The long-dashed line is from an extension of the PWBA by Basbas et al.[28] and yields a value for 160-keV protons of $\sigma_K = 3.0 \times 10^{-18}$ cm^2. The latter theory is a significant correction to the PWBA at proton energies lower than those of interest here, but this theory tends to underestimate experimental values of σ_K in the present range of interest through neglect of polarization effects.[29] The experimental Auger-electron yield curve in Fig. 4(a) follows, as expected, the general energy dependence of the cross-section curves shown in Fig. 4(b). The precision of measurement for Y is not good enough, however, to distinguish between the slightly different variations given by the three theories.

There are no known measurements of the L-shell ionization cross section σ_L for Al by protons. Therefore, we have taken recent Auger-yield measurements[30-32] of σ_L for Ar and scaled them[25,33] to obtain approximate values of σ_L for Al, as shown by the solid and dotted lines in Fig. 5(b). We have derived from these two curves an average "experimental" value of $\sigma_L = 3.9 \times 10^{-17}$ cm^2 for 160-keV protons on Al.

We also show in Fig. 5(b) calculated values of $\sigma_L^i (= \sigma_{L_1} + \sigma_{L_{23}})$ for Al from the BEA[25] (short-dashed line), the PWBA[34] (dot-dashed line), and the modified PWBA[35] (long-dashed line). These
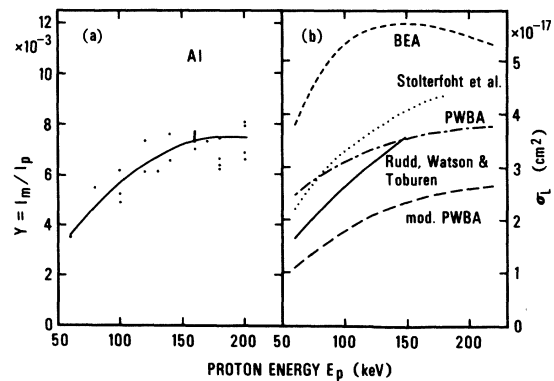

FIG. 5. (a) Variation of the Auger-electron yield Y $=I_m/I_p$ for Al as a function of proton energy E_p. The solid curve is a smooth curve through the experimental points. (b) Variation of σ_L for Al as a function of E_p. The short-dashed curve denoted BEA is calculated from the binary-encounter approximation (Ref. 25), the dot-dashed line denoted PWBA from the plane-wave Born approximation (Ref. 34), and the long-dashed line denoted mod. PWBA from the modified plane-wave Born approximation (Ref. 35). The other lines are derived cross sections for Al, as described in the text, from data for Ar measured by Stolterfoht et al. (Ref. 31) (the dotted line), and by Watson and Toburen (Ref. 30) and Rudd (Ref. 32) (the solid line).

curves yield values of σ_L at E_p =160 keV of 5.7 $\times 10^{-17}$ cm^2, 3.6×10^{-17} cm^2, and 2.4×10^{-17} cm^2, respectively. The PWBA and modified PWBA curves in Fig. 5(b) are of similar shape, but the BEA curve has its maximum at a lower value of E_p than the other two. The experimental yield data in Fig. 5(a) have a proton-energy dependence similar to the derived "experimental" values of σ_L and to the PWBA and modified PWBA curves in Fig. 5(b).

The precision and accuracy of the cross-section data shown in Figs. 4(b) and 5(b) are difficult to estimate. The imprecision of the original experimental data reported in these figures is about 10%, but the inaccuracy is estimated to be about 20%. Further, the use of the BEA to obtain σ_K for Be and σ_L for Al from σ_i data for other elements can result in additional systematic error. The accuracy of σ_i calculated with the use of the BEA, PWBA, and the modified PWBA is difficult to estimate due to the limited data available in the region of the maximum of the σ_i-vs-E_p curve. It does appear, however, that the BEA and PWBA provide a fairly good description of σ_i in the energy range of interest.[28,29,35] With the above discussion in mind, we have selected the values (at E_p =160 keV) of σ_K =6$\times 10^{-18}$ cm^2 for Be and σ_L =4.2$\times 10^{-17}$ cm^2 for Al shown in Table I and have assigned these σ_i values a possible inaccuracy (of unspecified sign) of 25%.

C. Evaluation of attenuation lengths and associated uncertainties

The measured absolute Auger-electron yields (determined by the procedure of Sec. IV A) for Be and Al at the proton energy of 160 keV are shown

in Table I together with the values of the other parameters needed to determine λ with the use of Eqs. (6) and (7). We also show estimates of the imprecision (probable error) of these quantities while estimates of the various sources of systematic error are listed in Table II. These estimates of error will be discussed before the attenuation lengths for Auger electrons in Be and Al are calculated.

The measurements of the Auger-electron yield, $Y = I_m/I_p$, had a probable error of about $\pm 10\%$, based on the precision of measurement of I_p, I_m, σ, k, and Z and on the variation of different measurements of Y. The limits of error in I_m due to background location and to the asymmetrical peak shape have been discussed in Sec. IV A.

We have assumed that the samples were microscopically smooth in the derivation of Eq. (6), but evaporated surfaces can be rough enough to cause a loss of electrons emitted in the direction of the analyzer.[36] Variations in surface roughness from sample to sample could lead to variations of Y greater than would be expected from the precision of measurement, but since the sample topography was not determined in these initial experiments, we could not establish the dependence of yield on roughness. It appears unlikely, however, that I_m would be reduced by more than about 10%–20% on going from an ideally smooth sample surface to Be or Al samples sequentially evaporated onto a metallic substrate.[36]

Proton bombardment of the samples can cause excitations in addition to inner-shell ionization, and such excitations can lead to the observation of "satellite" Auger-electron features of lower energy than the principal features.[10,25] For solid

TABLE II. Summary of sources of significant systematic errors and their estimated magnitude for the parameters used in Eq. (6) to determine electron attenuation lengths (Secs. IV A and IV C). A positive (negative) error indicates that the measured value of the parameter may be an overestimate (underestimate) of the true value by the percentage amount indicated.

Parameter	Estimated limits of systematic error
I_m (background under peak)	~ ± 5%
I_m (correction for inelastic scattering at peak)	~ ± 2%
I_m (non-Gaussian peak shape for high-energy portion of peak, σ)	~ ± 5%
I_m (peak asymmetry for Be)	~ ± 12½%
I_m (sample roughness)	~ −20%
I_m (satellite Auger peaks)	~ −10%
T (Moiré effects of grids, collection efficiency)	~ ± 5%
σ_i	~ ± 25%
N (sample morphology, voids)	~ −5%
G (alignment, solid angle of analyzer, beam position on sample)	~ ± 6%

samples, the satellite features (sometimes re-
ferred to as being due to intrinsic excitations)
would overlap the intensity associated with inelas-
tic scattering (referred to as being due to extrinsic
excitations). In principle, the satellite intensity
should be measured and added to I_m but, in prac-
tice, reliable separation of the background, intrin-
sic, and extrinsic intensities is difficult. How-
ever, the satellite intensity is believed to be
small ($\lesssim 10\%$) in the present work because of the
similarity in shape of the spectra in Fig. 3 and
those produced by electron excitation.[5,25]

The measurement of T has been described in
Sec. III. It is possible that Moiré effects could
cause directional variations of T, but no signifi-
cant variations ($> 5\%$) in the value of T at various
positions on the collector were observed during
separate calibration experiments.

Values of the atomic number density N in Table
I have been calculated assuming that the samples
had bulk density. It is possible that the presence
of voids and defects in the evaporated material
could lead to the film having an average density
about 5% less than the bulk value.[37] Although the
derived attenuation length is a function of N, the
total cross section for inelastic scattering ($= 1/N\lambda$)
is independent of N.

Values of the angles used to determine G have
an estimated inaccuracy and an imprecision of
about 1°. The inaccuracy arises in part from loca-
tion of the sample at the center of curvature of
the analyzer and the location of the proton beam;
the imprecision results from the reorientation of
the sample after an evaporation which could lead
to variation of the measured values of Y.

Finally, for the shells with electrons of low
binding energy of interest here, the fluorescent
yield ω is poorly known but is believed to be about
0.001.[4] We have, therefore, set ω equal to zero
in Eq. (6).

We have used the parameter values listed in
Table I to compute an attenuation length of 6.1 Å
for 100-eV electrons in Be and of 1.9 Å for 67-eV
electrons in Al. Each value has an imprecision
(probable error) of ±10% based on the probable
errors of the measured values of Y and T. The
estimates of possible systematic error listed in
Table II are somewhat speculative, and even for
those cases where the sign is believed known, we
have preferred not to apply any systematic cor-
rections to our λ values as correction factors
were not established in this preliminary experi-
ment. We can, however, estimate that the lower
and upper bounds of λ are 2.4 and 14.7 Å for Be
and 0.9 and 4.1 Å for Al, respectively. These
bounds have been determined by additively com-
bining the estimates of possible systematic error

(in each direction) and adding the estimated pro-
bable error (±10%) for each element.[38] These
errors are believed conservative in that we have
determined the combined systematic effects of
extreme values for all of the parameters. An al-
ternative procedure[38] is to combine the systematic
errors in quadrature to yield systematic errors
of +30% and −37% for Be and +28% and −35% for
Al. On this basis, the derived values of λ would
have an estimated probable error of ±10% and an
estimated systematic error of about ±35%.

The magnitude of the various sources of impre-
cision and inaccuracy in this experiment could be
minimized in the future. The Auger-electron inten-
sity could be determined more satisfactorily with
the background-subtraction technique and the in-
elastic-scattering correction method proposed by
Houston.[19] The measured yield should be cor-
related with measurements of the surface topo-
graphy.[39] Uncertainties in cross sections[24−35]
for ionization of particular subshells by proton
impact and in the corresponding fluorescent or
Coster-Kronig yields, however, may restrict this
measurement method to low-Z elements.

D. Comparison of attenuation-length values to published data

Table III lists the results from the present
experiment together with measured values for
similar electron energies reported by Seah[40] for
Be and by Tracy[41] for Al. Both of these latter
measurements were made by the "overlayer"
method.[1] The systematic errors associated with
this measurement technique have not been investi-
gated fully, but appear to be significant.[1,42] Al-
though the present results are lower than the other
measured values for Be and Al, this difference is
not significant in view of the possible systematic
error we have reported for this experiment (Sec.
IV C) and of the unknown uncertainties of the over-

TABLE III. Summary of numerical values of attenua-
tion lengths λ for Be at 100 eV and for Al at 67 eV. The
uncertainties for the present experiment are discussed
in the text.

| | λ (Å) | |
Source of data	Be	Al
Present experiment	6.1	1.9
Seah[a]	~8.6	
Tracy[b]		~3.7
Penn[c]	3.8	3.4

[a] Measured result of Seah (Ref. 40) for Be.
[b] Measured result of Tracy (Ref. 41) for Al.
[c] Calculated values derived from the theory of Penn
(Ref. 8).

layer experiments.

Table III also shows values of the attenuation length for Be and Al calculated by Penn.[8] His calculation was based on a free-electron model that implies plasmon excitation as the dominant inelastic-scattering mechanism, an assumption well justified for Be and Al. The calculated value for Be is less than, and the calculated value for Al is larger than, the respective values reported here.

Two considerations need to be kept in mind in making the above comparisons. First, an attenuation length measured in this experiment does not correspond necessarily to the constant attenuation length of an infinite medium that was implicitly assumed in the derivation of Eq. (6). For free-electron-like metals such as Be and Al, inelastic scattering by surface-plasmon excitation in the vicinity of the sample surface is an important energy-loss mechanism. The additional attenuation due to surface-plasmon excitation, however, is partially compensated by a reduction in the probability of volume-plasmon excitation.[43] Second, the derived attenuation lengths (Table III) are comparable to the corresponding crystal-lattice constants so that the analysis of Sec. II may not be valid on an atomic scale. Comparison of the attenuation lengths obtained here with the results of other experiments is of limited value until more is known about (a) electron transport on a microscopic scale and (b) the sources of systematic error in the experimental techniques used for previously reported data.[1,40-42]

V. SUMMARY

Measurements have been made of the absolute yields of characteristic KVV (100-eV) Auger electrons from Be and $L_{23}VV$ (67-eV) Auger electrons from Al when semi-infinite Be and Al samples were bombarded by 60- to 220-keV protons. These measurements have been used with a simple electron-transport model to derive effective values of the inelastic attenuation lengths for the Auger electrons in the surface regions of the two metals.

This experiment has the disadvantage that absolute measurements of Auger-electron intensity are required whereas only relative measurements of intensity are needed for other techniques that have been used to determine attenuation lengths.[1] The present method is subject to errors that are presently large but which could be reduced substantially in future work. This method does have the important advantage, however, that measurements are made on semi-infinite samples, thereby avoiding the uncertainties in film morphology and homogeneity that arise with the more commonly used overlayer method.

The attenuation lengths determined here are 6.1 Å for 100-eV electrons in Be and 1.9 Å for 67-eV electrons in Al. The transport model used to derive these values may not be valid in detail near (within several atomic layers of) the sample surface. Thus, the present values cannot necessarily be compared with attenuation lengths determined for the bulk solid although there is in fact reasonable agreement. Attenuation lengths determined by the present method are, however, particularly appropriate for use in quantitative surface analysis by AES and XPS because the same electron-measurement conditions and the same electron-transport model were used. Further measurements of the same type would be justified to provide empirical parameters for AES and XPS experiments and to search for any modifications of scaling relationships used for determining attenuation lengths in bulk matter.[8]

*Present address: Texas Instruments, P. O. Box 5936 Dallas, Tex. 75222.

[1]C. J. Powell, Surf. Sci. 44, 29 (1974).

[2]R. G. Musket and W. Bauer, Thin Solid Films 19, 69 (1973).

[3]P. B. Needham, Jr., T. J. Driscoll, C. J. Powell, and R. J. Stein, Appl. Phys. Lett. 30, 357 (1977).

[4]W. Bambynek, B. Crasemann, R. W. Fink, H.-U. Freund, H. Mark, C. D. Swift, R. E. Price, and P. V. Rao, Rev. Mod. Phys. 44, 716 (1972).

[5]R. J. Stein, C. J. Powell, P. B. Needham, Jr., and T. J. Driscoll (unpublished).

[6]C. J. Todd and R. Heckingbottom, Phys. Lett. A 42, 455 (1973); P. C. Kemeny, J. G. Jenkin, J. Liesegang, and R. C. G. Leckey, Phys. Rev. B 9, 5307 (1974).

[7]P. W. Palmberg, Anal. Chem. 45, 549A (1973); B. L. Henke, Phys. Rev. A 6, 94 (1972).

[8]D. R. Penn, J. Vac. Sci. Technol. 13, 221 (1976); J. Electron Spectrosc. 9, 29 (1976).

[9]L. C. Northcliffe and R. F. Schilling, Nuclear Tables

A $\underline{7}$, 233 (1970).

[10]W. E. Moddeman, T. A. Carlson, M. O. Krause, B. P. Pullen, W. E. Bull, and G. K. Schweitzer, J. Chem. Phys. $\underline{55}$, 2317 (1971).

[11]P. B. Needham, Jr., and B. D. Sartwell, Phys. Rev. A $\underline{2}$, 1686 (1970).

[12]J. C. Tracy and G. K. Bohn, Rev. Sci. Instrum. $\underline{41}$, 591 (1970).

[13]N. J. Taylor, Rev. Sci. Instrum. $\underline{40}$, 792 (1969).

[14]D. M. Zehner, N. Barbulesco, and L. H. Jenkins, Surf. Sci. $\underline{34}$, 385 (1973); H. G. Maguire and P. D. Augustus, Philos. Mag. $\underline{30}$, 95 (1974).

[15]C. J. Powell, Phys. Rev. Lett. $\underline{30}$, 1179 (1973).

[16]E. N. Sickafus, Rev. Sci. Instrum. $\underline{42}$, 933 (1971).

[17]J. E. Houston, Rev. Sci. Instrum. $\underline{45}$, 897 (1974).

[18]W. M. Mularie and W. T. Peria, Surf. Sci. $\underline{26}$, 125 (1971).

[19]J. E. Houston, J. Vac. Sci. Technol. $\underline{12}$, 255 (1975); H. H. Madden and J. E. Houston, J. Appl. Phys. $\underline{47}$, 3071 (1976).

[20]N. Swanson, J. Opt. Soc. Am. $\underline{54}$, 1130 (1964).

[21]N. Swanson and C. J. Powell, Phys. Rev. $\underline{167}$, 592 (1968).

[22]M. Terasawa, T. Tamura and H. Kamada, J. Phys. Soc. Jpn. $\underline{33}$, 1420 (1972).

[23]C. E. Dick and A. C. Lucas, Phys. Rev. A $\underline{2}$, 580 (1970).

[24]L. H. Toburen, in *Proceedings of the International Conference on Inner Shell Ionization Phenomena and Future Applications*, edited by R. W. Fink, S. T. Manson, J. M. Palms, and P. V. Rao (U.S. AEC, Technical Information Center, Oak Ridge, Tenn., 1973), CONF-720404, Vol. 2, p. 979.

[25]J. D. Garcia, R. J. Fortner, and T. M. Kavanagh, Rev. Mod. Phys. $\underline{45}$, 111 (1973).

[26]N. Stolterfoht, D. Schneider, and K. G. Harrison, Phys. Rev. A $\underline{8}$, 2363 (1973).

[27]G. S. Khandelwal, B.-H. Choi, and E. Merzbacher, Atomic Data $\underline{1}$, 103 (1969).

[28]G. Basbas, W. Brandt, and R. Laubert, Phys. Rev.

A $\underline{7}$, 983 (1973).

[29]W. Brandt, in *Atomic Physics 3*, edited by S. J. Smith and G. K. Walters (Plenum, New York, 1973), p. 155.

[30]R. L. Watson and L. H. Toburen, Phys. Rev. A $\underline{7}$, 1853 (1972).

[31]N. Stolterfoht, D. Schneider, and P. Ziem, Phys. Rev. A $\underline{10}$, 81 (1974).

[32]M. E. Rudd, Phys. Rev. A $\underline{10}$, 518 (1974).

[33]Experimental values of σ_L for Ar have been scaled to apply to Al on the assumption that the ionization cross sections fall on a "universal curve" when $\sigma_L U_L^2$ is plotted against E_p/U_L, where E_p is the proton energy and U_L is the L-shell binding energy (Ref. 25). As σ_{L_1} for Al is at most 16% of $\sigma_{L_{23}}$ in the proton energy range of interest here, as calculated by the BEA, the PWBA, and the modified PWBA, we have used the L_{23}-shell binding energies for Al and Ar to scale the cross sections.

[34]B.-H. Choi, E. Merzbacher, and G. S. Khandelwal, Atomic Data $\underline{5}$, 291 (1973).

[35]W. Brandt and G. Lapicki, Phys. Rev. A $\underline{10}$, 474 (1974).

[36]P. H. Holloway, J. Electron Spectrosc. Related Phenom. $\underline{7}$, 215 (1975).

[37]K. L. Chopra, *Thin Film Phenomena* (McGraw-Hill, New York, 1969).

[38]P. J. Campion, J. E. Burns, and A. Williams, *A Code of Practice For the Detailed Statement of Accuracy* (National Physical Laboratory, London, 1973), pp. 13-16; C. Eisenhart, Science $\underline{160}$, 1201 (1968).

[39]R. D. Young, Phys. Today $\underline{24}$, No. 11, 42 (1971).

[40]M. P. Seah, Surf. Sci. $\underline{32}$, 703 (1972).

[41]J. C. Tracy, J. Vac. Sci. Technol. $\underline{11}$, 280 (1974); and private communication.

[42]M. Šunjić, D. Šokčević, and J. W. Gadzuk, Jpn. J. Appl. Phys. Suppl. $\underline{2}$, Pt. 2, 753 (1974).

[43]R. H. Ritchie, Phys. Rev. $\underline{106}$, 874 (1957); P. Feibelman, Surf. Sci. $\underline{36}$, 558 (1973); G. D. Mahan, Phys. Status Solidi B $\underline{55}$, 703 (1973); M. Šunjić and D. Šokčević, Solid State Commun. $\underline{15}$, 165 (1974).